RIG-I-Mediated Antiviral Responses to Single-Stranded RNA Bearing 5'-Phosphates

ARTICLE *in* SCIENCE · DECEMBER 2006

Impact Factor: 33.61 · DOI: 10.1126/science.1132998 · Source: PubMed

RIG-I-Mediated Antiviral Responses to Single-Stranded RNA Bearing 5'-Phosphates
Andreas Pichlmair, *et al.*
Science **314**, 997 (2006);
DOI: 10.1126/science.1132998

Science (print ISSN 0036-8075; online ISSN 1095-9203) is published weekly, except the last week in December, by the American Association for the Advancement of Science, 1200 New York Avenue NW, Washington, DC 20005.

the transfection of the respective RNA isolates. To completely rule out the possibility that replication of RV was required to trigger an IFN response, we isolated full-length RNA from virions and assessed it for the induction of IFN expression. Transfection of purified RV RNA effectively stimulated IFN induction in HEK 293T cells, whereas dephosphorylation of the genomic RV RNA isolates completely abrogated the observed IFN response (Fig. 3D). Together, these results demonstrate that RIG-I directly recognizes genomic RNA from RV independently of replication.

We next performed in vitro binding assays, testing the ability of 5′-triphosphate RNA to pull down RIG-I. RNA oligonucleotides with 3′-terminal biotin tags were generated and coincubated with whole-cell lysate from HEK 293 cells overexpressing full-length RIG-I and truncated versions of RIG-I. Although the 5′-triphosphate biotin oligonucleotide (tri-G-AC-U-Bio) was able to immunoprecipitate full-length RIG-I, no or little pulldown was seen when truncated versions of RIG-I (RIG-I CARD2 and RIG-I ΔHelicase_C) were tested for binding of the triphosphate RNA (Fig. 4A, right panel). Purified RIG-IC was also efficiently pulled down by triphosphate RNA oligonucleotides (Fig. 4B, second lane), but not if the initial 5′-triphosphate group was enzymatically removed before coincubation (Fig. 4B, fourth lane). These results indicate that 5′-triphosphate RNA directly binds to full-length RIG-I, and therefore RIG-I is the direct receptor responsible for the recognition of 5′-triphosphate RNA.

Our results provide evidence that uncapped unmodified 5′-triphosphate RNA (now termed 3pRNA) is a well-defined molecular structure of viral nucleic acids that is detected by RIG-I in the cytosol of eukaryotic cells. Many of the RNA species in the cytosol of eukaryotes are known to lack a free 5′-triphosphate group, although all RNA transcripts generated in the nucleus of a eukaryotic cell initially contain a 5′-triphosphate. Matured Pol I–transcribed ribosomal RNAs (rRNAs) in the cytosol have a monophosphate group at the 5′ end (*12*). mRNAs and small nuclear RNAs transcribed by Pol II are capped with a 7-methyl-guanosine group that is attached to the 5′-triphosphate (*13*). All mature tRNAs (Pol III) have a 5′-monophosphate (*14*), as is likely to apply to 5S rRNA. U6 RNA receives a γ-monomethylphosphate cap structure after transcription (*15*). 7SL RNA (Pol III), however, has a triphosphate at the 5′ end and is present at high copy numbers in the cytosol. Therefore, the presence or absence of a 5′-triphosphate might not be the only structural feature of RNA responsible for the distinction of self and viral RNA. Eukaryotic RNA undergoes substantial posttranscriptional modifications. The host machinery that guides nucleoside modifications and 2′-O-methylation of the ribose backbone is located in the nucleus (*16*). Because most RNA viruses do not replicate in the nucleus, extensive modification of viral RNA seems unlikely.

The mRNAs of viruses infecting eukaryotic cells commonly contain 7-methyl-guanosine cap structures at their 5′ ends and polyadenylate tails at their 3′ ends. Nonetheless, in many viruses, RNA synthesis leads to transient cytosolic viral RNA intermediates with an uncapped 5′-triphosphate end. RNA transcripts of all positive-strand RNA viruses of the family Flaviviridae start with an uncapped 5′-triphosphate, and members of all of these virus genera were reported as being recognized by RIG-I (*2*, *3*, *17*). Segmented NSVs initiate genomic and the complementary antigenomic RNA replication by a primer-independent de novo mechanism resulting in a 5′-triphosphate–initiated transcript (*18*). NSVs with a nonsegmented genome, including the paramyxoviruses and rhabdoviruses, initiate both replication and transcription de novo leading to 5′-triphosphate RNA in the cytosol. Consequently, genomic RNA from NSVs per se is expected to trigger an IFN response without the need for replication and presumed dsRNA formation. All viruses in the picornavirus-like supergroup use an RNA-dependent RNA Pol that exclusively uses a protein as a primer for both positive- and negative-strand RNA production; as a consequence, during the life cycle of picornaviruses, uncapped triphosphorylated 5′ ends are absent (*19*). Thus, although RIG-I is expected to be involved in the detection of Flaviviridae and NSVs, it cannot detect picornaviruses.

References and Notes

1. M. Yoneyama *et al.*, *Nat. Immunol.* **5**, 730 (2004).
2. R. Sumpter Jr. *et al.*, *J. Virol.* **79**, 2689 (2005).
3. H. Kato *et al.*, *Nature* **441**, 101 (2006).
4. L. Alexopoulou, A. C. Holt, R. Medzhitov, R. A. Flavell, *Nature* **413**, 732 (2001).
5. S. Rothenfusser *et al.*, *J. Immunol.* **175**, 5260 (2005).
6. L. Gitlin *et al.*, *Proc. Natl. Acad. Sci. U.S.A.* **103**, 8459 (2006).
7. J. T. Marques *et al.*, *Nat. Biotechnol.* **24**, 559 (2006).
8. D. H. Kim *et al.*, *Nat. Biotechnol.* **22**, 321 (2004).
9. M. Kerkmann *et al.*, *J. Biol. Chem.* **280**, 8086 (2005).
10. V. Hornung *et al.*, *Nat. Med.* **11**, 263 (2005).
11. K. Brzozka, S. Finke, K. K. Conzelmann, *J. Virol.* **80**, 2675 (2006).
12. M. Fromont-Racine, B. Senger, C. Saveanu, F. Fasiolo, *Gene* **313**, 17 (2003).
13. A. J. Shatkin, J. L. Manley, *Nat. Struct. Biol.* **7**, 838 (2000).
14. S. Xiao, F. Scott, C. A. Fierke, D. R. Engelke, *Annu. Rev. Biochem.* **71**, 165 (2002).
15. R. Singh, R. Reddy, *Proc. Natl. Acad. Sci. U.S.A.* **86**, 8280 (1989).
16. W. A. Decatur, M. J. Fournier, *J. Biol. Chem.* **278**, 695 (2003).
17. T.-H. Chang, C.-L. Liao, Y.-L. Lin, *Microbes Infect.* **8**, 157 (2006).
18. G. Neumann, G. G. Brownlee, E. Fodor, Y. Kawaoka, *Curr. Top. Microbiol. Immunol.* **283**, 121 (2004).
19. Y. F. Lee, A. Nomoto, B. M. Detjen, E. Wimmer, *Proc. Natl. Acad. Sci. U.S.A.* **74**, 59 (1977).

20. This study was supported by grants from the Bundesministerium für Bildung und Forschung (Biofuture 0311896) and the Deutsche Forschungsgemeinschaft (HA 2780/4-1 and Sonderforschungsbereich 571) to G.H., a grant from the Sonderforschungsbereich 455 to K.C., two grants from the Förderprogramm für Forschung und Lehre (489 to V.H. and 2004/33 to S.K.), and by the Graduiertenkolleg 1202 of the Deutsche Forschungsgemeinschaft. This work is part of the thesis of J.E. and S.K. at the University of Munich. We thank S. Rothenfusser for critically reading the manuscript.

Supporting Online Material

www.sciencemag.org/cgi/content/full/1132505/DC1
Materials and Methods
SOM Text
Figs. S1 to S5
Table S1
References

14 July 2006; accepted 18 September 2006
Published online 12 October 2006;
10.1126/science.1132505
Include this information when citing this paper.

RIG-I–Mediated Antiviral Responses to Single-Stranded RNA Bearing 5′-Phosphates

Andreas Pichlmair,[1] Oliver Schulz,[1] Choon Ping Tan,[1] Tanja I. Näslund,[2] Peter Liljeström,[2] Friedemann Weber,[3] Caetano Reis e Sousa[1]*

Double-stranded RNA (dsRNA) produced during viral replication is believed to be the critical trigger for activation of antiviral immunity mediated by the RNA helicase enzymes retinoic acid–inducible gene I (RIG-I) and melanoma differentiation–associated gene 5 (MDA5). We showed that influenza A virus infection does not generate dsRNA and that RIG-I is activated by viral genomic single-stranded RNA (ssRNA) bearing 5′-phosphates. This is blocked by the influenza protein nonstructured protein 1 (NS1), which is found in a complex with RIG-I in infected cells. These results identify RIG-I as a ssRNA sensor and potential target of viral immune evasion and suggest that its ability to sense 5′-phosphorylated RNA evolved in the innate immune system as a means of discriminating between self and nonself.

The innate immune response to viral infection is characterized by the rapid production of a range of cytokines, most prominently type I interferons (IFN-α/β) (*1*). Specialized plasmacytoid dendritic cells (pDC) produce IFN-α/β when RNA or DNA viral

genomes in endosomes trigger toll-like receptors (TLRs) 7, 8, and 9 (*2*). Other cell types rely on cytoplasmic virus sensors such as the RNA helicases RIG-I and MDA5 (*3*–*7*), which are believed to be activated by dsRNA produced during viral replication or convergent transcription of viral genes (*8*). Viral recognition pathways can be targeted as a means of immune escape (*9*). For example, influenza A virus NS1 protein suppresses IFN-α/β production in animal models, cell lines, and primary cells (*10*), including conventional (nonplasmacytoid) dendritic cells (cDC), a critical cell type for the induction of adaptive immunity (*11*, *12*). NS1 possesses an RNA binding domain at the N terminus (*13*) and some evidence suggests that it exerts its suppressive effect by sequestering dsRNA (*10*).

[1]Immunobiology Laboratory, Cancer Research UK, London Research Institute, London WC2A 3PX, UK. [2]Department of Microbiology, Tumor and Cell Biology, Karolinska Institutet, Stockholm 17177, Sweden. [3]Department of Virology, University of Freiburg, Freiburg 79104, Germany.

*To whom correspondence should be addressed. E-mail: caetano@cancer.org.uk

To address whether this is the case, we first confirmed that influenza A virus (A/PR/8/34 strain) inhibits IFN-α/β production through the action of NS1. cDC derived from murine bone marrow progenitors (BM-DC) (*14*) infected with a mutant virus lacking the protein (ΔNS1) produced 100 times more IFN-α than did cells infected with the parental wild-type strain (Fig. 1A) (*11*, *12*). This was independent of the TLR7-TLR8-TLR9 adaptor MyD88 (Fig. 1A), suggesting that the effect occurred by means of the cytoplasmic pathway. We then assessed the extent to which dsRNA is generated during influenza replication. Consistent with recent data (*15*), no dsRNA was detected in BM-DC or in more permissive Vero cells (Fig. 1, B and C, and fig. S1) with either ΔNS1 or the wild-type virus, even though the cells were uniformly infected (fig. S2). In contrast, dsRNA was detectable upon transfection with poly inosinic:cytidylic acid (poly I:C), a synthetic dsRNA, or infection with encephalomyocarditis virus (EMCV), a picornavirus (Fig. 1, B and C, and fig. S1). We next examined the ability of NS1 to inhibit responses to Semliki Forest virus (SFV), which, similar to EMCV, generates high levels of dsRNA (*16*). Cells infected with a recombinant SFV encoding NS1 (SFV-NS1) expressed NS1 protein (fig. S3), but produced levels of IFN-α comparable to cells infected with a control recombinant virus or wild-type SFV (Fig. 1D). Similarly, transfection with NS1 had no effect on the induction of an IFN-β reporter in response to EMCV or SFV, although it potently inhibited the response to ΔNS1 influenza or Sendai virus (SeV) (Fig. 1E) (*13*). Notably, the latter two viruses generate minimal levels of dsRNA (Fig. 1, B and C) (*15*), but induce high levels of IFN-α (Fig. 1, A and E, and fig. S4), whereas EMCV and SFV induce high levels of dsRNA (Fig. 1, B and C, and fig. S3) (*16*), but lower levels of IFN-α (Fig. 1E and fig. S4). Collectively, these data indicate that neither IFN-α induction nor the inhibitory effect of NS1 correlates with the presence of dsRNA.

SeV and ΔNS1 influenza are recognized by RIG-I, whereas EMCV is recognized by MDA5 (*6*, *7*). Therefore, we investigated whether the virus-specific effects of NS1 reflected its ability to interact with RIG-I. Consistent with this possibility, RIG-I tagged with green fluorescent

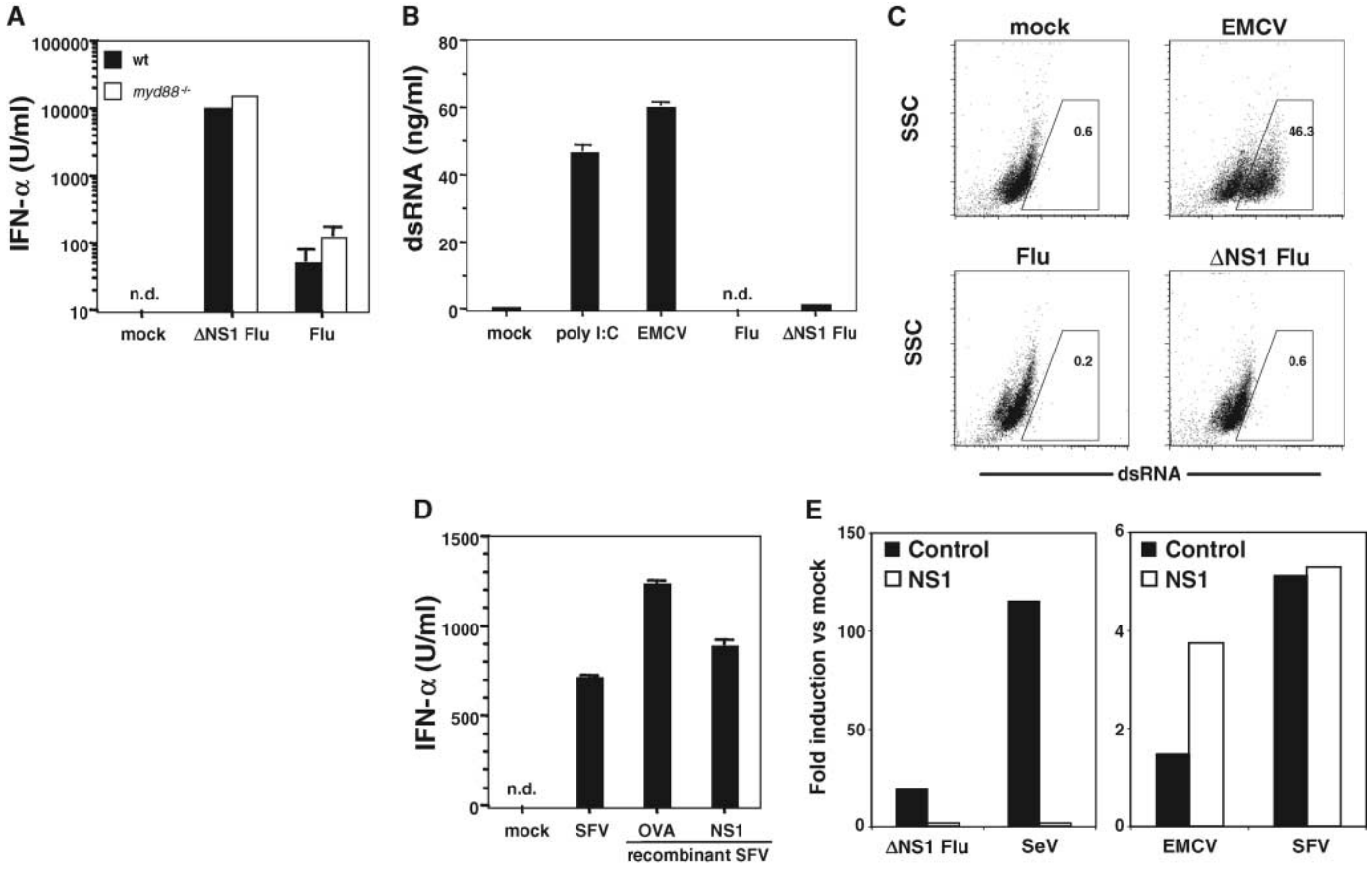

Fig. 1. Neither NS1 inhibition nor the induction of IFN-α/β correlates with viral dsRNA. (**A**) BM-DC from C57BL/6 (wt) or *myd88*$^{-/-}$ mice were cultured overnight in medium alone (mock) or with wild-type or ΔNS1 influenza virus. Data are average IFN-α levels of triplicate samples. (**B** and **C**) dsRNA in Vero cells 6 hours after infection with influenza virus or EMCV or after transfection with poly I:C measured by enzyme-linked immunosorbent assay (B) or flow cytometry (C). Numbers in (C) indicate the percentage of cells in gate. SSC, side scatter. (**D**) Same as (A), but cells were infected with wild-type SFV or recombinant SFV encoding NS1 or an irrelevant protein [ovalbumin (OVA)]. (**E**) Induction of luciferase activity in human embryonic kidney (HEK) 293 cells cotransfected with IFN-β reporter plasmids together with NS1-encoding plasmid or control empty vector and subsequently infected with the indicated viruses. Error bars in (A), (B), and (D) show means + SD. n.d., none detectable.

protein (GFP) or a hemagglutinin peptide (HA) coprecipitated with NS1 from postnuclear lysates of influenza-infected cells (Fig. 2, A and B). In addition, the cytoplasmic fraction of NS1 colocalized with GFP–RIG-I in infected cells (Fig. 2C). In contrast, MDA5 did not associate with NS1 in infected cells (Fig. 2B). These results suggest that NS1 selectively targets RIG-I rather than dsRNA during influenza virus infection.

Given the lack of dsRNA in infected cells, we addressed whether RIG-I might be activated directly by the influenza ssRNA genome. Transfection with genomic RNA extracted from influenza virions (flu vRNA) induced potent activation of the IFN-β reporter (Fig. 3A) and production of IFN-α and interleukin (IL)–6 by BM-DC at levels comparable or superior to those obtained by transfection with poly I:C (Fig. 3C). This was not due to the generation of progeny virus because flu vRNA transfection did not result in viral replication (Fig. 3B), consistent with the evidence that vRNA from negative strand viruses is not infectious (*17*). The response to flu vRNA was RIG-I dependent, given that it was inhibited by dominant negative RIG-I or by small interfering RNA (siRNA)–mediated knockdown of RIG-I in either mouse or human cells (Fig. 3D and fig. S5). RIG-I blocked responses to SeV but not EMCV (Fig. 3D), as expected (*6*), confirming the specificity of RIG-I reduction. NS1 suppressed the response to flu vRNA, and this was partly relieved by two point mutations previously reported to attenuate NS1 binding to RNA (*18*) (mutNS1, Fig. 3A). Finally, the addition of purified RIG-I to flu vRNA led to the formation of complexes with high molecular weight (Fig. 3E), demonstrating that RIG-I directly binds the influenza genome. Thus, RIG-I recognizes influenza ssRNA genomes and signals for cytokine production unless suppressed by NS1.

Mouse mRNA, total mammalian RNA [consisting of ~70% ribosomal RNA (rRNA)], and mammalian or bacterial tRNA did not elicit IFN responses (fig. S6), suggesting that RIG-I recognition is specific for viral RNA. Influenza vRNA is uncapped (*17*), and phosphorylated 5′

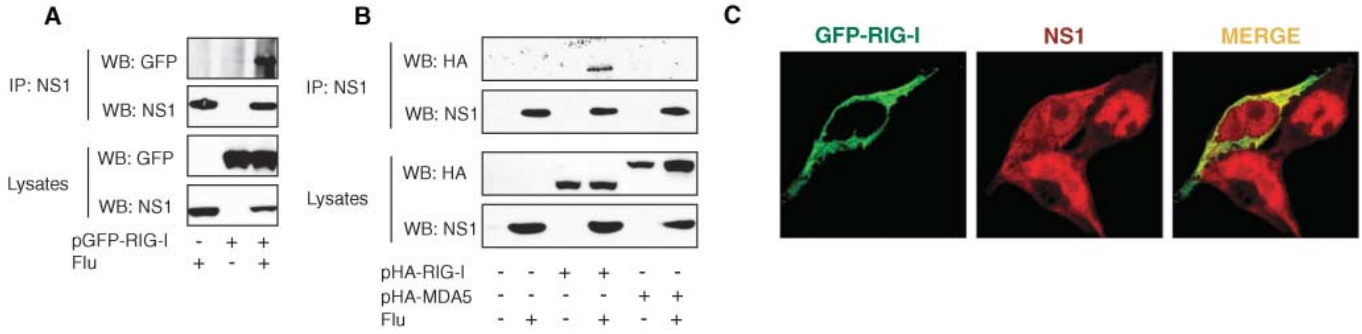

Fig. 2. The NS1 protein of influenza A virus interacts with RIG-I but not MDA5. (**A** and **B**) 293T cells were transfected with pGFP–RIG-I (A) or with pHA–RIG-I or pHA-MDA5 (B), and 12 hours later they were infected or not infected with influenza virus, as indicated. At 24 hours, cells were lysed and analyzed by Western blot (WB) for the presence of NS1 and GFP (A) or NS1 and HA (B) in total cell lysates (lower panels) or after immunoprecipitation (IP) with an antibody to NS1 (upper panels). (**C**) 293T cells were transfected with GFP–RIG-I, infected with influenza virus at 16 hours, and stained for NS1 at 24 hours. Shown are GFP–RIG-I, NS1, and the merged image.

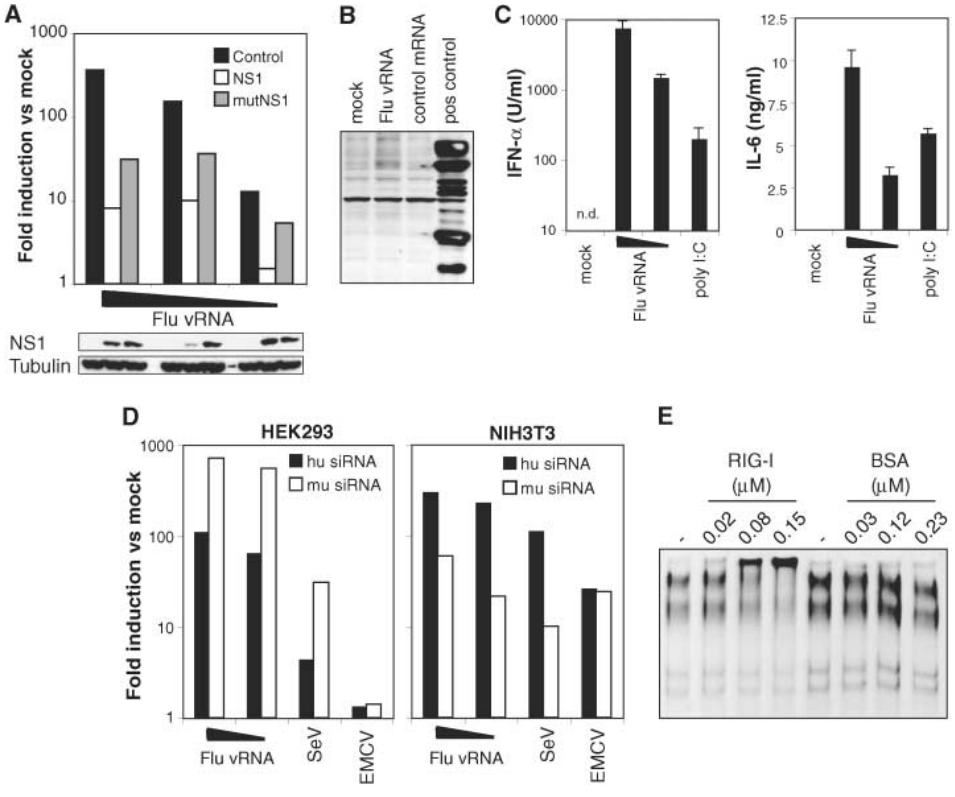

Fig. 3. Influenza vRNA triggers innate responses in a RIG-I–dependent manner. (**A**) HEK293 cells were cotransfected with IFN-β reporter plasmids and NS1 expression plasmid (NS1 or mutNS1) or empty vector (control). After 24 hours, cells were transfected with flu vRNA (0.2, 0.04, or 0.008 μg) and luciferase activity was measured at 38 hours. Western blots show the presence of NS1 or tubulin. (**B**) Lysates from cells transfected with flu vRNA or control mouse mRNA were probed with polyclonal antibody against influenza proteins. Influenza-infected cells served as positive (pos) control. (**C**) IFN-α and IL-6 accumulation in overnight culture supernatants from BM-DC that were mock treated or transfected with flu vRNA (1 and 0.2 μg) or poly I:C (0.5 μg). n.d., none detectable. Error bars show means + SD. (**D**) Inhibition of responses to flu vRNA by RIG-I reduction. Human HEK293 cells and mouse NIH 3T3 cells were cotransfected with IFN-β reporter plasmids and siRNAs specific for mouse or human RIG-I. After 72 hours, cells were transfected with flu vRNA (0.2 or 0.04 μg) or were infected with SeV or EMCV. Luciferase activity was measured at 86 hours. (**E**) Cold electrophoretic mobility shift assay analysis of RIG-I and flu vRNA interaction. Flu vRNA (1.08 nM) was incubated with the indicated concentrations of purified FLAG–RIG-I or bovine serum albumin (BSA) and resolved by electrophoresis. RNA was visualized by SYBR Green staining.

termini present in siRNA and ssRNAs generated by in vitro transcription have been reported to induce IFN-α/β when transfected into cells (*19*). We confirmed the latter observation (fig. S7) and tested whether flu vRNA recognition similarly depends on the presence of 5′-phosphates. Treatment with calf intestinal phosphatase (CIP) completely abrogated the stimulatory properties of flu vRNA (Fig. 4, A and B). This was due to phosphatase activity rather than nonspecific effects of CIP, given that it could be blocked by inorganic phosphate or EDTA (fig. S8). Furthermore, CIP did not affect the ability of vRNA to stimulate TLR7-dependent IFN-α production from pDC-containing cell populations (fig. S8). Vesicular stomatitis virus (VSV) also has an uncapped genome (*17*) and is recognized by RIG-I (*6*). Similar to influenza, transfection with VSV vRNA induced an IFN response, which was completely abrogated by previous CIP treatment (Fig. 4, C and D). Consistent with the evidence that EMCV is not recognized by RIG-I (*6*, *7*), EMCV vRNA failed to induce a response when transfected into cells at amounts comparable to flu or VSV vRNA (Fig. 4C). These data suggest that cells use RIG-I to respond to the phosphorylated 5′ termini of uncapped ssRNA viral genomes.

Finally, we assessed whether 5′ phosphorylation contributes to RIG-I binding. In vitro transcribed RNA formed a complex with RIG-I in cell lysates, which was less resistant to salt extraction when the RNA was pretreated with CIP (Fig. 4E). In vitro binding assays that used purified RIG-I confirmed that complexes with CIP-treated RNA were less stable (fig. S9). Notably, the addition of control but not CIP-treated RNA to cell lysates promoted the formation of a complex containing NS1 and RIG-I (Fig. 4F), mimicking the association seen in infected cells (Fig. 2). RIG-I associated only weakly with the NS1 mutant (mutNS1, Fig. 4F), which binds ssRNA poorly when compared with wild-type protein (fig. S10). Thus, RIG-I preferentially forms stable complexes with RNA that contains phosphorylated 5′ ends and NS1 is recruited to such complexes at least in part through its RNA binding domain.

The ability to sense viral presence is critical for initiating innate and adaptive immunity to viral infection. We found that virus recognition can be accomplished by RIG-I–mediated sensing of ssRNA viral genomes bearing 5′-phosphates. This can be blocked by viral antagonists such as the NS1 protein of influenza A virus, which is found in a complex with RIG-I (supporting online material text). Our results demonstrate that the repertoire of antiviral defense strategies includes the detection of cytoplasmic ssRNA, explaining how some viruses that produce little or no dsRNA (*15*) can be efficiently recognized, even before viral replication (*20*). Consistent with the evidence that RIG-I can bind to dsRNA in vitro (*4*, *5*), our data do not exclude the possibility that the complex of RIG-I and ssRNA is stabilized by the presence of intramolecular double-stranded regions, such as the panhandle structures that are found at the ends of the influenza genome (*17*). However, this is not sufficient to induce RIG-I activation unless the ssRNAs also contain phosphorylated 5′ termini. Notably, many RNA viruses have uncapped RNAs bearing 5′-triphosphates. In picornaviruses, a notable exception, the vRNA is covalently linked to a small protein, VPg (*17*), perhaps explaining why EMCV cannot be recognized by RIG-I (*6*, *7*). The 5′-phosphates are also absent from self-mRNA as a result of the addition of a 7-methyl-guanosine cap and may be largely inaccessible in rRNA and tRNA, through association with ribosomal proteins or formation of cloverleaf structures containing 3′ overhangs. Thus, the cytoplasmic presence of RNA containing accessible 5′-phosphates allows discrimination between self and viral RNA, indicating that, similar to dsRNA, 5′ phosphate–bearing ssRNA constitutes a viral "pathogen-associated molecular pattern" (*21*). This finding, added to the recent discovery of innate sensing of cytoplasmic DNA (*22*–*24*), suggests a parallel

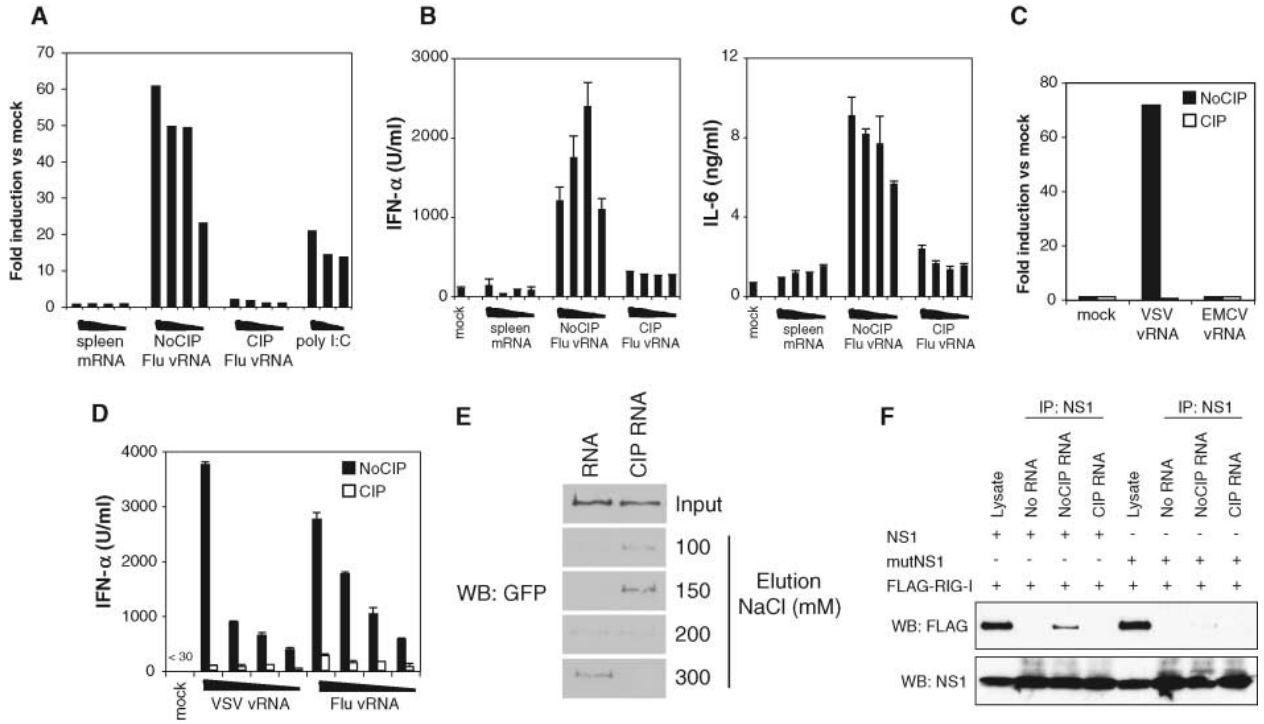

Fig. 4. ssRNAs containing phosphorylated 5′ ends bind RIG-I and activate antiviral responses. HEK293 cells transfected with IFN-β reporter and Renilla luciferase control plasmids (**A** and **C**) or BM-DC (**B** and **D**) were transfected with different amounts (0.6, 0.2, 0.06, or 0.02 μg) of mouse spleen mRNA or flu vRNAs, or with vRNA from 8×10^7 plaque-forming units VSV (C) or fivefold serial dilutions thereof (D). RNAs were pretreated with CIP or not (NoCIP). Luciferase activity [(A) and (C)] or IFN-α and IL-6 [(B) and (D)] were measured after overnight culture. (**E**) In vitro transcribed biotinylated RNA was treated with or without CIP, bound to streptavidin beads, and incubated with lysates from 293T cells transfected with GFP–RIG-I. Data show protein eluted from the beads by washing with buffer containing the specified NaCl concentrations. (**F**) Lysates of 293T cells cotransfected with pFLAG–RIG-I and pCAAGS-NS1 or pCAAGS-mutNS1 were incubated with or without 7SK-as RNA that had been either mock or CIP treated. After immunoprecipitation (IP) with the antibody to NS1, the presence of RIG-I and NS1 was analyzed by Western blot (WB).

between cytosolic and endosomal viral recognition, with MDA5, RIG-I, and the cytosolic DNA receptor constituting functional homologs of TLR3, TLR7, TLR8, and TLR9. Similar to virologists, the innate immune system may therefore have learned to classify viruses by their genomes.

References and Notes

1. A. N. Theofilopoulos, R. Baccala, B. Beutler, D. H. Kono, *Annu. Rev. Immunol.* **23**, 307 (2005).
2. T. Kawai, S. Akira, *Nat. Immunol.* **7**, 131 (2006).
3. M. Yoneyama *et al.*, *Nat. Immunol.* **5**, 730 (2004).
4. M. Yoneyama *et al.*, *J. Immunol.* **175**, 2851 (2005).
5. S. Rothenfusser *et al.*, *J. Immunol.* **175**, 5260 (2005).
6. H. Kato *et al.*, *Nature* **441**, 101 (2006).
7. L. Gitlin *et al.*, *Proc. Natl. Acad. Sci. U.S.A.* **103**, 8459 (2006).
8. B. L. Jacobs, J. O. Langland, *Virology* **219**, 339 (1996).
9. A. Garcia-Sastre, C. A. Biron, *Science* **312**, 879 (2006).
10. A. Garcia-Sastre, *Virology* **279**, 375 (2001).
11. S. S. Diebold *et al.*, *Nature* **424**, 324 (2003).
12. A. Fernandez-Sesma *et al.*, *J. Virol.* **80**, 6295 (2006).
13. X. Wang *et al.*, *J. Virol.* **74**, 11566 (2000).
14. Materials and methods are available as supporting material on *Science* Online.
15. F. Weber, V. Wagner, S. B. Rasmussen, R. Hartmann, S. R. Paludan, *J. Virol.* **80**, 5059 (2006).
16. O. Schulz *et al.*, *Nature* **433**, 887 (2005).
17. D. Knipe, P. M. Howley, Eds., *Fields Virology* (Lippincott Williams & Wilkins, Philadelphia, PA, ed. 4, 2001).
18. W. Wang *et al.*, *RNA* **5**, 195 (1999).
19. D. H. Kim *et al.*, *Nat. Biotechnol.* **22**, 321 (2004).
20. S. E. Collins, R. S. Noyce, K. L. Mossman, *J. Virol.* **78**, 1706 (2004).
21. C. A. Janeway Jr., *Cold Spring Harb. Symp. Quant. Biol.* **54**, 1 (1989).
22. Y. Okabe, K. Kawane, S. Akira, T. Taniguchi, S. Nagata, *J. Exp. Med.* **202**, 1333 (2005).
23. K. J. Ishii *et al.*, *Nat. Immunol.* **7**, 40 (2006).
24. D. B. Stetson, R. Medzhitov, *Immunity* **24**, 93 (2006).

25. This work was funded by Cancer Research UK. We thank I. Kerr for SFV and EMCV, T. Muster for ΔNS1, J. Skehel for purified influenza, S. Diebold for flu vRNA isolation and GFP RNA synthesis, A. Bergthaler for VSV vRNA, J. Yewdell for the antibody to NS1, C. Basler for FLAG–RIG-I, and A. Garcia-Sastre for NS1 constructs. We are grateful to members of the Immunobiology Laboratory for support.

Supporting Online Material

www.sciencemag.org/cgi/content/full/1132998/DC1
Materials and Methods
SOM Text
Figs S1 to S10
References

25 July 2006; accepted 2 October 2006
Published online 12 October 2006;
10.1126/science.1132998
Include this information when citing this paper.

Direct Measurement of the Full, Sequence-Dependent Folding Landscape of a Nucleic Acid

Michael T. Woodside,[1,2] Peter C. Anthony,[3] William M. Behnke-Parks,[2] Kevan Larizadeh,[2] Daniel Herschlag,[4] Steven M. Block[2,5]*

Nucleic acid hairpins provide a powerful model system for understanding macromolecular folding, with free-energy landscapes that can be readily manipulated by changing the hairpin sequence. The full shapes of energy landscapes for the reversible folding of DNA hairpins under controlled loads exerted by an optical force clamp were obtained by deconvolution from high-resolution, single-molecule trajectories. The locations and heights of the energy barriers for hairpin folding could be tuned by adjusting the number and location of G:C base pairs, and the presence and position of folding intermediates were controlled by introducing single-nucleotide mismatches.

Elucidating the mechanisms by which proteins and nucleic acids fold into three-dimensional structures is key to developing insights into biomolecular function (*1*), improving predictive models (*2*, *3*), and understanding the basis of diseases linked to misfolding (*4*). For more than two decades, free-energy landscape formalisms have provided the fundamental conceptual framework for describing folding (*5*). Numerous experimental and theoretical studies have probed specific features of folding landscapes, including the properties of transition states (*6*), intermediate states (*7*), and the ruggedness of the energy surface (*8*). Experiments, however, have characterized only limited aspects of the folding landscape, such as the locations and heights of energy barriers and how these barriers change when perturbed by solvent substitutions, temperature jumps, substrate changes, or mutations (*9*). Direct measurements of the shape of an energy landscape at all points along the reaction coordinate have not been feasible. Here, we show how the full energy landscape for the formation of a nucleic acid hairpin can be derived from sufficiently high-resolution trajectories of single-molecule folding.

Single nucleic-acid hairpins subjected to mechanical loads provide a powerful model system for investigating energy landscapes and understanding the effects of primary and secondary structure on folding (*10*–*13*). The molecular end-to-end extension is recorded during the folding transition and supplies a natural reaction coordinate that can be related directly to the number of bases paired in the hairpin stem. Previous work has characterized specific aspects of the folding landscape. In particular, short hairpins tend to fold as simple, two-state systems (*10*, *13*), indicative of a single-transition energy barrier. Conventional analysis of single-molecule records supplies the free-energy difference between the folded and unfolded states, as well as the height and location of the barrier (*10*). For hairpins with random (unpatterned) stem sequences, the barrier is typically located close to the unfolded state, with a height controlled largely by the size of the loop (*13*). However, finer details of the folding landscape have been heretofore inaccessible, due to limited spatial and temporal resolution, as well as instrumental baseline drift. Using a high-bandwidth, passive force clamp with an ultra-stable dumbbell assay (*14*), we have now been able to reconstruct the shape of the landscape.

Sets of DNA hairpins were synthesized in which the heights and locations of energy barriers were systematically varied, as well as the numbers and locations of any folding intermediates. Sequences were designed based on a model of the sequence-dependent energy landscape derived from the thermodynamic and mechanical properties of nucleic acids (*13*, *15*). Both ends of the hairpins were attached to long handles of double-stranded DNA (dsDNA) (*13*) bound specifically to polystyrene beads held in a dumbbell configuration by two independently controlled optical traps (Fig. 1A). A constant force, F, was applied with a force clamp (*14*), and high-resolution trajectories of the end-to-end extension (~0.1 nm/$\sqrt{\text{Hz}}$) were recorded for a range of forces. The extensions of folded, unfolded, and any intermediate states were measured directly from these records. The locations and heights of energy barriers between these states were computed from the force-dependence of the state lifetimes (*10*, *13*). These measurements of specific points on the landscape were then taken as benchmarks for an experimental determination of the free energy at every point along the reaction coordinate, deconvolving the measured probability distribution of hairpin extension to correct for blurring effects arising from thermal motions associated with the beads and the DNA tether.

A typical record of extension under load (Fig. 1B) shows two-state folding behavior: Two nearly Gaussian peaks in the extension histogram correspond to the folded and unfolded states. Here, $F \approx F_{1/2}$, the load at which the hairpin spends equal time in each state. The lifetimes of the folded (τ_f) and unfolded (τ_u) states depend exponentially on F according to $\tau_f(F) \propto$

[1]National Institute for Nanotechnology, National Research Council of Canada, Edmonton AB, Canada, T6G 2M9. [2]Department of Biological Sciences, [3]Biophysics Program, [4]Department of Biochemistry, [5]Department of Applied Physics, Stanford University, Stanford, CA 94305, USA.

*To whom correspondence should be addressed. E-mail: sblock@stanford.edu